Multigenerational Cortical Inheritance of the Rax2 Protein in Orienting Polarity and Division in Yeast

Tracy Chen,[1] Takatoshi Hiroko,[2] Amitabha Chaudhuri,[1] Fumika Inose,[2] Matthew Lord,[1] Shigeko Tanaka,[2] John Chant,[1]* Atsushi Fujita[2]*

Diploid yeast cells repeatedly polarize and bud from their poles, probably because of highly stable marks of unknown composition. Here, Rax2, a membrane protein, was shown to behave as such a mark. The Rax2 protein itself was inherited immutably at the cell cortex for multiple generations, and Rax2 was shown to have a half-life exceeding several generations. The persistent inheritance of cortical protein markers would provide a means to couple a cell's history to the future development of a precise morphogenetic form.

Bud site selection and the resulting formation of axes of cytoskeletal polarization serve as a paradigm for developing a mechanistic understanding of how cells develop asymmetry in response to spatial cues. Yeast cells polarize and divide by budding in two patterns: the axial pattern of haploid **a** or α cells, and the bipolar pattern of diploid **a**/α cells (*1–4*). These patterns are observed by viewing of cells growing on a solid surface (*1*) or by staining of division scars (*3–5*) (Fig. 1A). Haploid-specific expression of *AXL1* is the basis for the haploid-diploid switch between budding patterns (*6*).

In the axial pattern, buds form immediately adjacent to the previous site of cell division, as marked by a group of proteins (septins, Bud3, Bud4, and Bud10/Axl2) that congregate at the neck late in the cell cycle to be passed on to progeny, thereby defining axial positions of polarization (*7–10*). Their actions are transient in that these marks then dissipate. Little is known concerning the composition of the bipolar marks. Physiological experiments have indicated that these markers are different from the axial markers in that they are long-lived, perhaps persisting for several generations (*4*).

RAX2 was identified through a mutant hunt in which an *axl1* strain, which buds in the bipolar pattern (*6*), was mutagenized and examined for isolates defective for the bipolar pattern (*11*). *RAX2* is predicted to encode

[1]Department of Molecular and Cellular Biology, Harvard University, 7 Divinity Avenue, Cambridge, MA 02138, USA. [2]National Institute of Bioscience & Human Technology, AIST 1-1 Higashi, Tsukuba 305-8566, Japan.

*To whom correspondence should be addressed. E-mail: chant@fas.harvard.edu (J.C.) and atsushi@nibh.go.jp (A.F.).

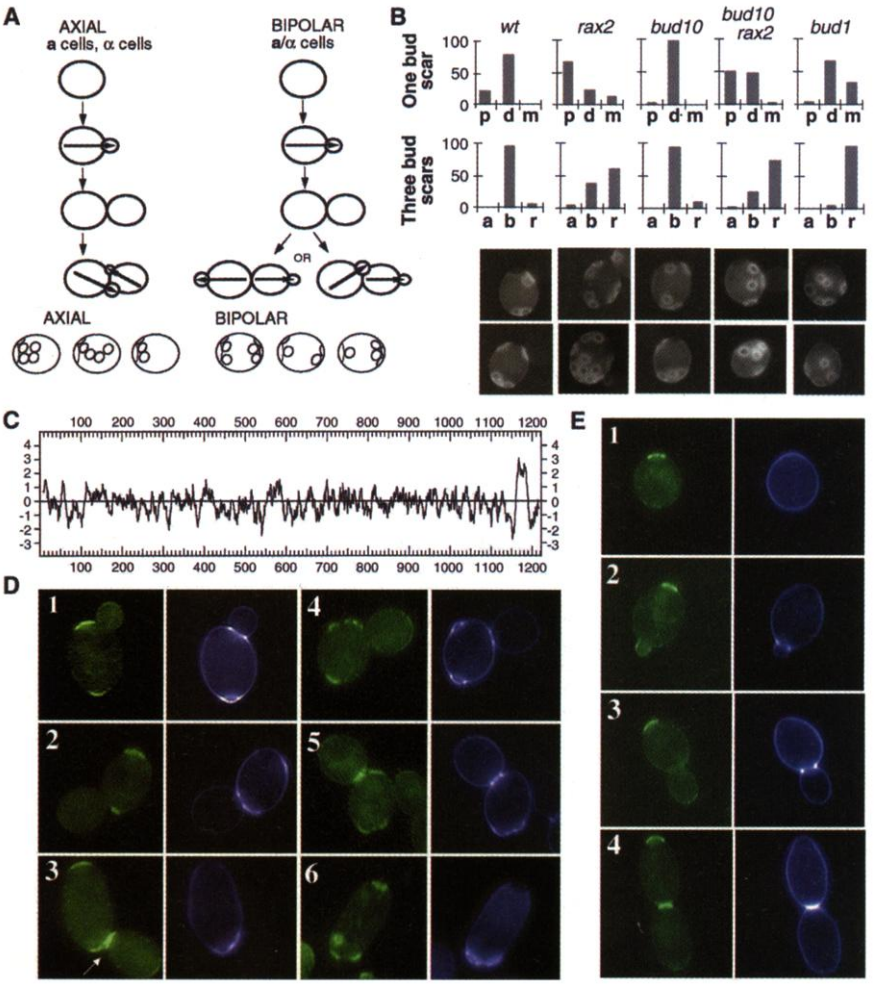

Fig. 1. Budding patterns and the Rax2 protein. (**A**) The axial and bipolar patterns of budding, as viewed by growth on solid support (upper panel) (*1–3*) and by staining of bud scars (lower panel) (*4, 6*). Upper panel: Arrows within cells indicate axes of polarity. Lower panel: All cells exhibit one birth scar, the point at which a cell was originally attached to its mother (larger structure at pole) and zero to multiple bud scars (smaller circles). In the axial pattern, the bud scars form a chain that begins at the birth scar. In the bipolar pattern, clusters of scars typically form at both cell poles (*4*). (**B**) Effects of *rax2* mutations on bipolar bud site selection. All analyses were performed in homozygous diploids. Quantitation was performed as follows (*4*). The first bud scar was scored as being at the birth scar–proximal pole (p), at the birth scar–distal pole (d), or in the midsection of the cell (m). For the three-bud-scar stage, bud scars were scored as axial (a) if all were connected in a chain with at least one touching the birth scar; bud scars were scored as bipolar (b) if all three were at the distal pole, one or more scars were at each pole, or all scars were at the proximal pole with a noticeable separation between them. Scars were scored as being random (r) if one or more scars were in the midsection of the cell. Representative micrographs are shown. In all panels, more than 200 cells were counted. Strains: HAB251-15B, JC1984, TC257, TC254, and Y324 (*11*). (**C**) The Rax2 hydrophobicity profile: amino acid number plotted versus relative hydrophobicity (*18*). (**D**) In diploid cells, Rax2-GFP rings decorate previous division sites. Green, Rax2-GFP; blue, division scars. Strain: TC230 (*11*). (**E**) Cell cycle timing of Rax2 arrival in the mother-bud neck. Strain: TC230 (*11*). Note that in the micrographs of (B), (D), and (E), birth scars are oriented upward. Cell numbers in (D) and (E) are discussed in the text.

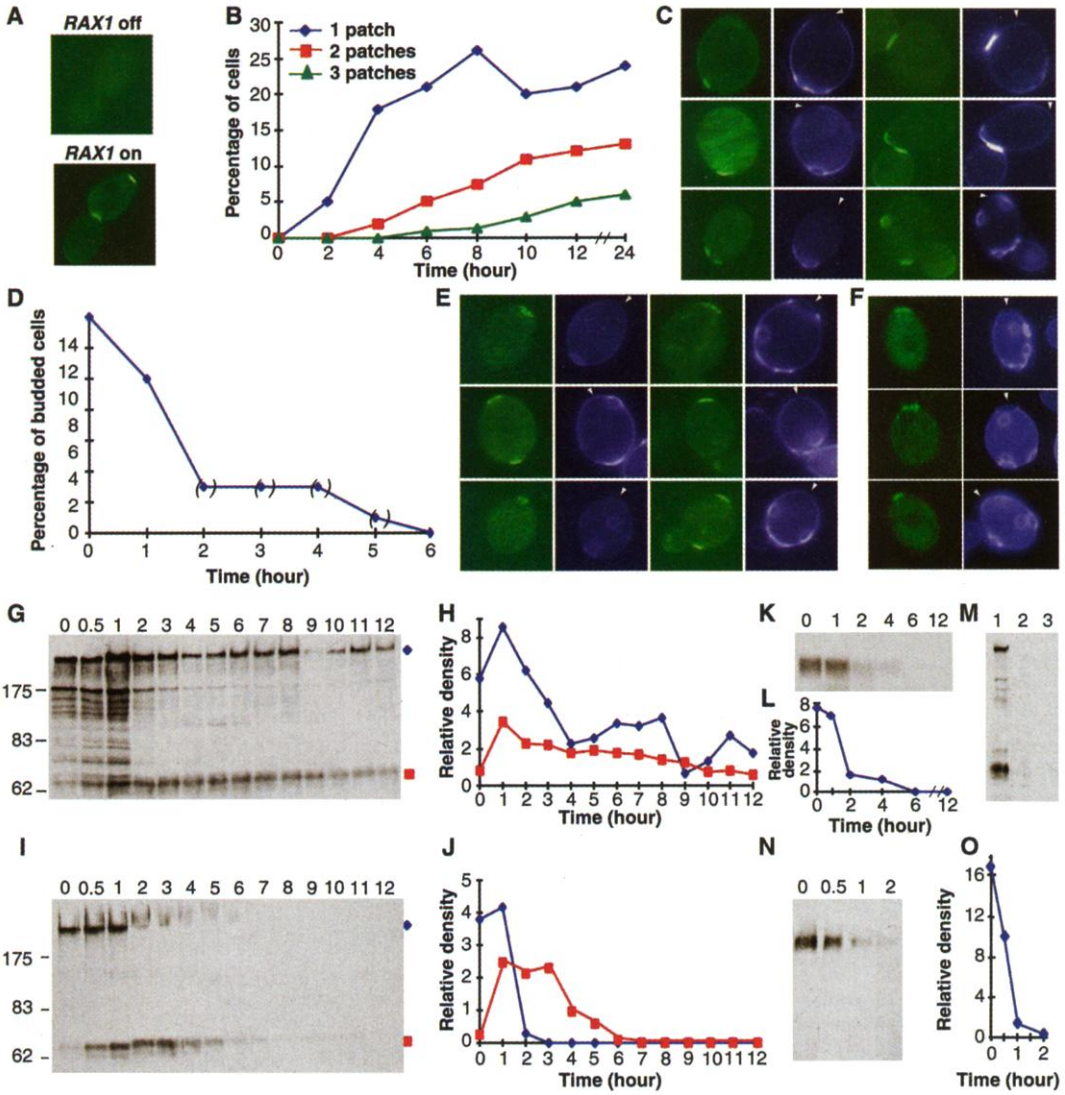

Fig. 2. Rax2 behaves as an inherited protein. (**A**) *RAX1* expression is required for the delivery of Rax2-GFP to the cell surface. *RAX1* is expressed from the *GAL1* promoter. *RAX1* off: Transcription is repressed (glucose medium). *RAX1* on: Transcription is induced (galactose medium). Strain: TC276 (*11*). (**B**) An induction time course of Rax2-GFP production. Cells were grown under repressing conditions and then *RAX1* was induced (time zero), allowing Rax2-GFP to transit to the cell surface. The percentage of cells showing a ring or rings of Rax2-GFP on their cell surface was scored. (**C**) Rax2-GFP and division scars are shown after 5 hours of induction (*11*). Birth scars are highlighted with a small arrowhead. (**D**) A repression time course of functional Rax2-GFP production. Cells were grown under inducing conditions, and then *RAX1* was repressed. The percentage of cells showing a collar of Rax2-GFP associated with the mother-bud neck is shown. At 2 hours onward, all neck-associated Rax2-GFP signals were greatly diminished in intensity, as denoted by bracketed data points. (**E**) Rax2-GFP and division scars are shown after 6 hours of repression (*11*). (**F**) Examples of cells are shown after 18 hours of repression. (**G** to **J**) A time course of Rax2-Myc stability in the insoluble (G) and soluble fractions (I) after repression of the *GAL1-RAX2* construct. Strain: JC1984 carrying pGAL-RAX2-MYC (*11*). Quantitative data from scanning of (G) and (I) are shown in (H) and (J). (**K** and **L**) A Northern blot showing the decay of RAX2 mRNA during a repression time course of the *GAL1-RAX2* construct under conditions identical to those in (G) to (J). (**M**) Expression and repression of Rax2 production from the *GAL1* promoter under steady-state conditions (*GAL1-RAX2*). Western blot detection of Rax2-Myc is shown. Lane 1, growth on galactose (inducing); lane 2, growth on glucose (repressing); lane 3, control, no construct. Strain: JC1984 carrying pGAL-RAX2-MYC or vector (*11*). (**N** and **O**) A time course of Bud10-Myc stability after repression from the *GAL1-BUD10* construct. Strain: HAB251-15B carrying pGAL-BUD10-MYC (*11*).

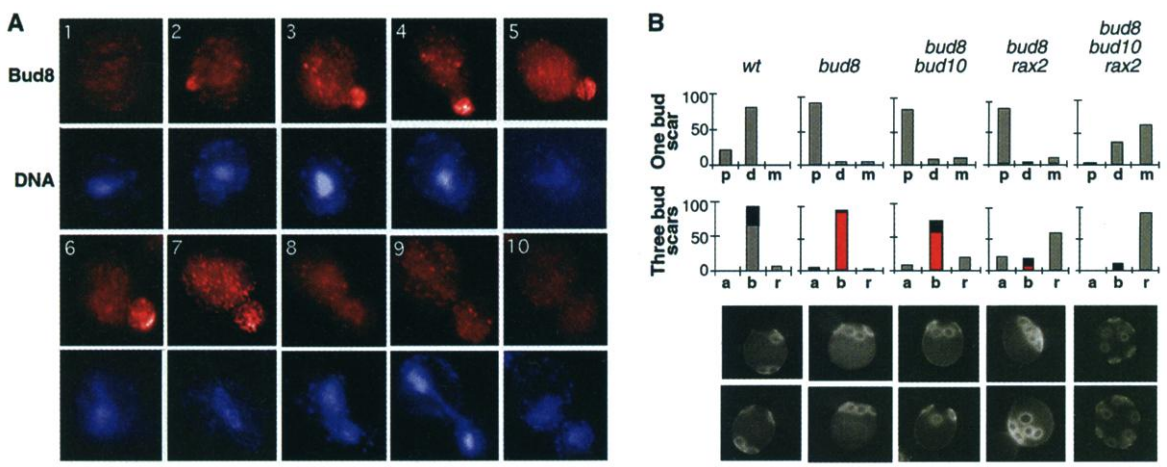

Fig. 3. The subcellular localization of Bud8 and its effects on bud site selection. (**A**) The cell cycle timing of Bud8-Myc localization. Strain: TC467 (*11*). (**B**) The effects of *bud8* mutations on bipolar bud site selection in homozygous diploids. Notation for scores is the same as in Fig. 1B. Bipolar budding in the three-scar count is further categorized as proximal bipolar (red; all scars at proximal end, characteristic of the *bud8* phenotype), bipolar with bud scars at both ends (black), and distal bipolar (gray; all bud scars at distal end). Strains: TCb83, TC362, TC398, and TC380 (*11*).

a novel type 2 membrane-spanning protein (Fig. 1C). A homolog is evident in fission yeast, but none is apparent in higher cells. *rax2* null mutations disrupt the bipolar pattern of *axl1* haploid cells without affecting the axial pattern of otherwise wild-type haploids (*11*). Examination of diploids showed that *RAX2* is required for the bipolar pattern under normal circumstances (Fig. 1B). The *rax2* phenotype is complicated by the recent observation that when the bipolar marks are perturbed, the axial landmarks, normally silent in diploids, can become active (*12, 13*). To eliminate ambiguity, we examined a *rax2* strain defective for the axial marker Bud10 (Fig. 1B). The bipolar pattern remained defective, indicating that the Rax2 protein has a direct role in producing the bipolar pattern.

Detailed analysis of the *rax2* phenotype showed an important feature. *RAX2* was required for the maintenance of the bipolar pattern, but not for its establishment: *rax2/rax2 bud10/bud10* cells chose their first bud sites at their poles with 98% efficiency, versus 100% in the wild type (Fig. 1B, one-bud-scar count), but subsequent budding events occurred in much more random fashion (72% random at three-bud-scar stage, versus 5% random in the wild type). These data support a mechanistic distinction between the placement of the first bipolar bud site on the newborn daughter and the placement of subsequent sites, whereby other factors are responsible for the selection of the first bud site on the newborn daughter (*12*).

To analyze Rax2 location, we made a functional chromosomal *RAX2-GFP* (green fluorescent protein) fusion. In **a**/α cells producing Rax2-GFP, we observed one or more cell surface rings of Rax2-GFP (Fig. 1D). Each ring was associated with a completed division site, as marked by a birth or bud scar. Rax2 localization fits well with Rax2's role in the maintenance of the bipolar pattern: Division scars mark the poles, and old division sites act as foci for guiding bipolar bud site selection (*4*).

The formation of new Rax2 rings occurred late in the cell cycle. For most of the cell cycle, no Rax2 signal was seen in association with the mother-bud neck (Fig. 1E, cells 2 and 3), although rings marking previous division sites remained present. Just before cytokinesis, a concentration of Rax2-GFP formed at the mother-bud neck (Fig. 1E, cell 4). The Rax2-GFP ring split at cytokinesis (Fig. 1D, cell 3, arrow), endowing each progeny cell with a Rax2 ring.

The observed localization suggested the possibility that Rax2 rings were deposited in the mother-bud neck during each cell cycle and then inherited, giving rise to cells decorated by multiple rings (an "inheritance mechanism"). The alternate possibility is that Rax2 has affinity for a component of previous division sites and diffuses until interacting with a binding site (an "affinity mechanism"). These two localization hypotheses can be distinguished by a system that allows induction or repression of functional Rax2 production. *RAX2* expression from an inducible promoter was not used, because cell cycle–specific transcription of *RAX2* (*13–15*) appears important for precise Rax2 localization. We proceeded as follows. We first determined that Rax1 was required for the delivery of Rax2 through the secretory pathway en route to the cell surface (Fig. 2A). Placing *RAX1* under an inducible promoter (*GAL1*) allowed inducible cell surface accumulation of Rax2 (Fig. 2A) while retaining the cell cycle periodicity of *RAX2* expression.

To distinguish experimentally whether an inheritance or affinity mechanism produced Rax2 localization, we performed an induction time course. New Rax2 rings formed in mother-bud necks after 2 hours of induction (Fig. 2B). As induction proceeded, cells with one Rax2 ring accumulated, then cells with two rings, then three, and so on—consistent with the inheritance mechanism of localization. We examined cells with a sufficient number of division scars such that some must have been present before induction. Such cells showed Rax2-GFP localization at only a subset of scars (Fig. 2C), most likely those sites formed after induction. As a confirmation of this view, the cell's oldest division site, marked by the birth scar, was never labeled on such cells (Fig. 2C). These observations strongly argue that an inheritance mechanism is operating. In marked contrast to our observations, an affinity mechanism predicts that all division sites, new and old, should become labeled simultaneously.

To test whether Rax2 rings are enduring as predicted by an inheritance mechanism of localization, we performed a repression time course. Effective repression of Rax2-GFP production occurred by 2 hours of repression, as indicated by a sharp decrease in the frequency of cells exhibiting nascent Rax2-GFP rings at their necks (Fig. 2D). Those present were very faint. After several hours of effective repression, old cells retained bright rings of Rax2-GFP associated with a subset of division sites (Fig. 2E); these are most likely older division sites because new Rax2 was not being delivered to the cell surface. In confirmation of this view, all birth scars (marking the first division site) were labeled on these cells (Fig. 2E). In a longer repression time course of 18 hours, we observed cells with many division scars that exhibited labeling of only their birth scars (Fig. 2F). Thus, Rax2-GFP rings can be inherited for several generations.

If Rax2 rings are inherited, one would predict Rax2 to be a long-lived protein. To address this issue, we expressed *RAX2* from the *GAL1* promoter and then repressed its expression. Full-length Rax2 and a shortened form were present in both insoluble and soluble pools (Fig. 2, G to J). The insoluble forms of Rax2 were very stable, with a half-life of about 6 hours (Fig. 2, G and H). Rax2 protein even remained detectable 24 hours after repression of its expression (*13*). The control protein Bud10 disappeared rapidly after repression (Fig. 2, N and O). Thus, Rax2 is a highly stable protein, consistent with our cytological observations.

If Rax2 contributes to the maintenance of the bipolar pattern but not its establishment, how are the poles initially specified for budding in the newborn daughter? *BUD8* and *BUD9* are required for the selection of polar bud sites on newborn daughters (Fig. 3B) (*12*). We attempted to localize Bud8 and Bud9. A consistent Bud9 signal was not observed, presumably because of low expression levels. Bud8 was readily observed as specifically localizing to the surfaces of small buds and tips of larger buds (Fig. 3A). Localized signal dissipated before cytokinesis. Bud tip localization is consistent with *BUD8*'s role in directing the first bud site to the tip of the newborn diploid daughter (*12*).

The localizations of Bud8 and Rax2 may explain how each contributes to the bipolar budding pattern. A newborn daughter endowed with a ring of Rax2 at its birth pole (Fig. 1E, cell 1) is guided by Bud8 to form its first bud at the distal pole (Fig. 1E, cells 2 and 3). As the bud matures, a second Rax2 ring is laid down at the distal pole (Fig. 1E, cell 4) of the now once-budded cell, resulting in a cell with Rax2 rings at both poles. These Rax2 rings are now properly positioned to guide subsequent budding to the poles to maintain bipolar budding.

Rax2 rings contribute to the maintenance of the bipolar pattern of budding, and these rings remain unaltered on the surfaces of cells for multiple generations, possibly for a cell's lifetime. As such, Rax2 represents an example of epigenetic inheritance. A number of forms of epigenetic inheritance are known, including organellar genomes and prion-type elements (*16*). Rax2 inheritance is perhaps most similar to the epigenetic inheritance of orientation in rows of cilia in *Paramecium* (*17*), the molecular basis of which has not been investigated. We anticipate that inherited protein marks at the cell cortex will be found to contribute to the development of intricate tissue architecture in higher eukaryotes as well.

References and Notes

1. D. Freifelder, *J. Bacteriol.* **80**, 567 (1960).
2. J. B. Hicks, J. N. Strathern, I. Herskowitz, *Genetics* **85**, 373 (1977).
3. J. Chant, I. Herskowitz, *Cell* **65**, 1203 (1991).
4. J. Chant, J. R. Pringle, *J. Cell Biol.* **129**, 751 (1995).
5. J. R. Pringle, *Methods Enzymol.* **194**, 732 (1991).

6. A. Fujita *et al.*, *Nature* **372**, 567 (1994).
7. J. Chant *et al.*, *J. Cell Biol.* **129**, 767 (1995).
8. S. L. Sanders, I. Herskowitz, *J. Cell Biol.* **134**, 413 (1996).
9. T. Roemer, K. Madden, J. Chang, M. Snyder, *Genes Dev.* **10**, 777 (1996).
10. A. Halme, M. Michelitch, E. L. Mitchell, J. Chant, *Curr. Biol.* **6**, 570 (1996).
11. For supplementary data, as well as more information about strains, plasmids, and methods used, see *Science* Online (www.sciencemag.org/cgi/content/full/290/5498/1975/DC1).
12. J. E. Zahner, H. A. Harkins, J. R. Pringle, *Mol. Cell. Biol.* **16**, 1857 (1996).
13. T. Chen, J. Chant, unpublished data.
14. R. J. Cho *et al.*, *Mol. Cell* **2**, 65 (1998).
15. P. T. Spellman *et al.*, *Mol. Biol. Cell* **9**, 3273 (1998).
16. R. B. Wickner, *Science* **264**, 566 (1994).
17. J. Beisson, T. M. Sonnenborn, *Proc. Natl. Acad. Sci. U.S.A.* **53**, 275 (1965).
18. J. Kyte, R. F. Doolitle, *J. Mol. Biol.* **157**, 105 (1982).
19. We thank C. Richardson for early contributions to this work, members of both laboratories for scientific support, R. Losick for comments on the manuscript, and N. Green, Y. Kikuchi, and Y. Koyama for helpful discussions. Supported by NIH grant GM49782 (J.C.) and by a Human Frontiers of Science Fellowship (M.L.).

3 August 2000; accepted 3 November 2000

Rescue of Photoreceptor Degeneration in Rhodopsin-Null *Drosophila* Mutants by Activated Rac1

Hui-Yun Chang and Donald F. Ready*

Rhodopsin is essential for photoreceptor morphogenesis; photoreceptors lacking rhodopsin degenerate in humans, mice, and *Drosophila*. Here we report that transgenic expression of a dominant-active *Drosophila* Rho guanosine triphosphatase, Drac1, rescued photoreceptor morphogenesis in rhodopsin-null mutants; expression of dominant-negative Drac1 resulted in a phenotype similar to that seen in rhodopsin-null mutants. Drac1 was localized in a specialization of the photoreceptor cortical actin cytoskeleton, which was lost in rhodopsin-null mutants. Thus, rhodopsin appears to organize the actin cytoskeleton through Drac1, contributing a structural support essential for photoreceptor morphogenesis.

Sensory neurons present a challenge for morphogenesis: to harness the generic mechanisms of the cytoskeleton to shape a cell to the needs of its specific sensory protein. For photoreceptors, it is clear that morphogenesis and maintenance of the photosensitive organelle, the rhabdomeres of *Drosophila* and the outer segments vertebrate rods and cones, depend on their sensory protein, rhodopsin (*1*–*3*). Rhabdomeres and outer segments are orderly stacks of photosensitive plasma membrane organized from enormously expanded apical cell surfaces. The forces that constrain this expansion and organize it into a dense stack are incompletely understood, but the cortical actin cytoskeleton and its associated proteins are substantial contributors (*4*, *5*). We suggest that in addition to its sensory role, *Drosophila* rhodopsin organizes the cortical actin cytoskeleton into an essential morphogenetic constraint (*6*), the rhabdomere terminal web (RTW). The RTW defines the regular, curving base of the rhabdomere that partitions the rhabdomere from the photoreceptor cytoplasm. In rhodopsin-null mutants, the rhabdomere base fails to organize correctly, and the rhabdomere collapses deep into the photoreceptor cytoplasm in convoluted sheets of apposed membrane (*1*).

Department of Biological Sciences, Purdue University, West Lafayette, IN 47907, USA.

*To whom correspondence should be addressed. E-mail: dready@bilbo.bio.purdue.edu

A chimeric protein that decorates F-actin with green fluorescent protein (GFP) (*7*) revealed the RTW as bundled microfilaments extending from the rhabdomere base deep into the photoreceptor (Fig. 1). Before rhodopsin expression, the RTW of developing photoreceptors showed less microfilament bundling, resembling a house painter's brush (Fig. 1C). At about 90% of pupal development (pd), after the onset of rhodopsin expression at 75% pd, RTW microfilaments elongated commensurate with the increasing microvillar length and gathered into bundles (Fig. 1D).

RTW maturation and rhabdomere morphogenesis fail in photoreceptors lacking rhodopsin. Paralleling the normal initiation of microvillar organization observed in rhodopsin-null mutants, the RTW of mutant photoreceptors appeared normal before the time when rhodopsin expression would normally commence (Fig. 1E). The RTW growth and bundling that normally follow rhodopsin expression failed in rhodopsin-null photoreceptors (Fig. 1F). Unlike wild-type rhabdomeres (Fig. 2A), the smaller, flattened rhabdomeres formed in the rhodopsin-null mutant collapsed into the photoreceptor cytoplasm in convoluted sheets of apposed membrane during the first day after eclosion (Fig. 2B). The actin cytoskeleton becomes thoroughly disorganized in the absence of rhodopsin.

Although rhodopsin contributes about 50% of rhabdomere membrane protein (*8*), it is unlikely to support morphogenesis by a simple mass effect. Smaller, but ultrastructurally normal rhabdomeres form in mutants in which Rh1 is reduced by over 99% (*9*). Furthermore, a pulse of rhodopsin expression restricted to a narrow window of development is sufficient to rescue rhabdomere morphogenesis in photoreceptors otherwise lacking rhodopsin (*10*). We propose that an additional role for rhodopsin is to contribute an activity required to organize the RTW into an effective subapical barrier.

Rho family guanosine triphosphatases (GTPases), which include Rho, Rac, and Cdc42, have emerged as key regulators of the actin cytoskeleton (*11*). Like their Ras cousins, they cycle between inactive guanosine diphosphate– and active guanosine triphosphate–bound forms and mediate signals from membrane receptors to downstream effectors that can modify actin-associated proteins and thereby regulate cytoskeletal architecture and dynamics. Profound defects of morphogenesis result from perturbation of Rho family signaling (*12*–*14*). G protein–coupled membrane receptors, including rhodopsin family members, have been shown to regulate the Rho family (*15*), raising the possibility that rhodopsin contributes to rhabdomere morphogenesis through Rho family GTPases.

Drosophila Rac1, Drac1, localized to the rhabdomere base beginning with the onset of microvillar organization during midpupal development (Fig. 3A); it remained subapical in adult eyes (Fig. 3B). To explore potential Drac1 functions in rhabdomere morphogenesis, we expressed dominant-negative N17Drac1 at defined stages of eye development. N17Drac1 expression during rhabdomere morphogenesis led to reduced, disordered rhabdomeres (Fig. 2C). Fewer microvilli were seen in cross section, and a well-defined rhabdomere base was not formed; apposed sheets of rhabdomere membrane involuted into the photoreceptor cytoplasm. Although these defects were reminiscent of those seen in rhodopsin-null mutants, the phenotype was not a consequence of a failure of rhodopsin delivery to the rhabdomeres (Fig. 4C). The actin cytoskeleton, however, appeared diffuse and disordered as a result of transgene expression (Fig. 4C).

The resemblance of the rhabdomere base defects caused by N17Drac1 to those seen in